arXiv:1112.0172v1 [astro-ph.CO] 1 Dec 2011

The broad Fe Kα line and supermassive black holes

Predrag Jovanović[a,*]

[a] *Astronomical Observatory, Volgina 7, 11060 Belgrade, Serbia*

Abstract

Here we present an overview of some of the most significant observational and theoretical studies of the broad Fe Kα spectral line, which is believed to originate from the innermost regions of relativistic accretion disks around central supermassive black holes of galaxies. The most important results of our investigations in this field are also listed. All these investigations indicate that the broad Fe Kα line is a powerful tool for studying the properties of the supermassive black holes (such as their masses and spins), space-time geometry (metric) in their vicinity, their accretion physics, probing the effects of their strong gravitational fields, and for testing the certain predictions of General Relativity.

Keywords: galaxies: active, black holes, accretion and accretion disks, X-ray emission spectra
PACS: 98.54.-h, 98.62.Js, 98.62.Mw, 78.70.En

---

1. Supermassive black holes

According to General Relativity (Einstein, 1916), a black hole (named by Wheeler, 1968) is a region of space-time around a collapsed mass with a gravitational field that has became so strong that nothing (including electromagnetic radiation) can escape from its attraction, after crossing its event horizon (Wald, 1984). The problem of such catastrophic gravitational collapse was first adressed by Chandrasekhar (1931) when he discovered the upper mass limit for ideal white dwarfs, composed of a degenerate electron-gas. Subsequent studies by Landau (1932); Oppenheimer & Snyder (1939) and Penrose (1965) established the modern theory of gravitational collapse. The theory of black holes, as well as their fundamental properties are presented in numerous monographs and papers (see e.g. Carter, 1973; Chandrasekhar, 1983), and therefore in this review we will focus only on those studies which are necessary for the discussion of the relation between black holes and the Fe Kα spectral line.

All black holes in nature are commonly classified according to their masses as: supermassive black holes (with masses $M_{BH} \sim 10^5 - 10^{10}\ M_\odot$), intermediate-mass black holes ($M_{BH} \sim 10^2 - 10^5\ M_\odot$), stellar-mass black holes ($M_{BH} < 10^2\ M_\odot$), mini and micro black holes ($M_{BH} \ll M_\odot$). A crucial event for the acceptance of black holes was the discovery of pulsars by Hewish et al. (1968), because it was the clear evidence of the existence of neutron stars, and therefore, confirmation of Chandrasekhar limit. The first detection of a solar mass black hole came in 1972, when the mass of the rapidly variable X-ray source Cygnus X-1 was proven to be above the maximum allowed for a neutron star (see e.g. Ferrarese & Ford, 2005, and references therein).

Nowadays, it is widely accepted that supermassive black holes are located in the centers of most of galaxies, and thus have a fundamental influence on galactic formation and evolution. Some of the first indirect arguments that they exist in galactic nuclei are given by Lynden-Bell (1969) and Lynden-Bell & Rees (1971). Also, according to the unification model of active galactic nuclei – AGN (Antonucci, 1993; Peterson, 1997; Krolik, 1999), they are most likely powered by the accretion of gas onto their central supermassive black holes with mass ranging from 10^5 to $10^9\ M_\odot$ (Kaspi et al., 2000; Peterson et al., 2004).

1.1. Space-time geometry in vicinity of supermassive black holes

In general, black holes have three measurable parameters (not including the Hawking temperature): charge, mass (and hence gravitational field) and angular momentum (or spin). In the case of supermassive black holes, only the latter two are of sufficient importance because they are responsible for several effects which can be observationally detected (for more details see e.g. Jovanović & Popović, 2008).

A central supermassive black hole of a galaxy can be stationary or rotating. In the first case, space-time geometry in the black hole vicinity depends only on its mass M and is described by the Schwarzschild metric (Schwarzschild, 1916), while in the latter case, space-time geometry depends also on spin a (i.e. angular momentum $J = aM$) of the black hole and is described by Kerr metric (Kerr, 1963). Therefore, Schwarzschild metric describes the spherically symmetric gravitational field around a time-steady non-rotating black hole in vacuum, while the Kerr metric describes the gravitational field outside an uncharged rotating black hole and, contrary to the Schwarzschild metric, is no longer spherically symmetric. Boyer & Lindquist (1967) discovered a generalized coordinate system in which Kerr metric is most commonly used today (see e.g. Carter, 1973).

---

[*] Corresponding author
Email address: `pjovanovic@aob.bg.ac.rs` (Predrag Jovanović)

Several characteristic radii can be defined around black holes, and the most important are (see e.g. Jovanović & Popović, 2009): 1. Schwarzschild radius $R_S = 2GM/c^2$ (representing the limiting radius below which a collapsed mass form a spherically symmetric non-rotating black hole), where G is the gravitational constant and c is the speed of light; 2. gravitational radius R_g (being a half of R_S and usually used as a unit for distance around a black hole); 3. radius of event horizon R_h (representing space-time boundary below which events cannot affect an outside observer); and 4. radius of marginally stable orbit R_{ms} (representing the minimum allowed radius of a stable circular equatorial orbit around a black hole).

The equations governing photon trajectories in the Kerr metric are derived by Carter (1968). Misner et al. (1973) showed that certain relativistic effects in vicinity of a black hole, such as light banding, gravitational and Doppler shifts as seen by distant observer could be computed by solving the equation of the photon orbit. Cunningham & Bardeen (1972, 1973) calculated radiation of a point source in a circular orbit in the equatorial plane around an extreme Kerr metric black hole (see Fig. 1).

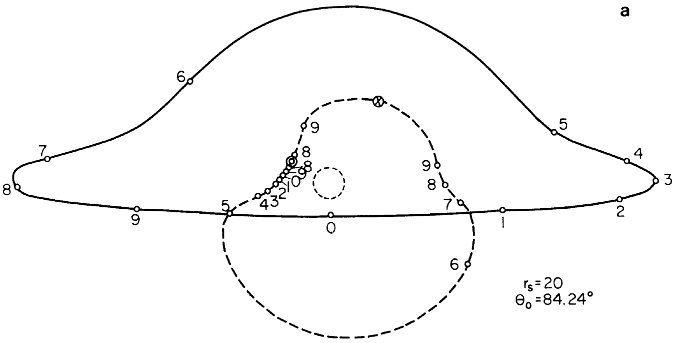

Figure 1: A circular orbit (solid line) of a point source in the equatorial plane around an extreme Kerr metric black hole. Image Credit: Cunningham & Bardeen, Copyright: ApJ, 183, 237 (1973).

Bardeen (1970) studied the effects of accretion from a disk of gas orbiting a black hole on its properties, and showed that the Kerr metric is more appropriate for describing supermassive black holes than the Schwarzschild metric. This conclusion is strengthened even more by Thorne (1974), who showed that a black hole at the center of an accretion disk would be spun up to the maximum possible value of $a \approx 0.998$ in a relatively short time. In such a case the disk would be extended down to about 1.23 R_g, while in the case of a non-rotating black hole it could extend only down to 6 R_g.

1.2. Accretion onto the supermassive black holes

Some observed quasars have luminosities of up to $L_{bol} \sim 10^{47}$ erg/s (Schneider, 2006). The corresponding total energy emitted during the lifetime of such quasars can be estimated to $E \geq 3 \times 10^{61}$ erg, assuming that their minimum age is about 10^7 years and that their luminosities do not change significantly over the lifetime (Schneider, 2006). Accretion is the only mechanism which can yield sufficient efficiency ϵ (defined as the mass fraction of fuel that is converted into energy, according to $E = \epsilon mc^2$) to explain such high energies. The maximum efficiency of accretion is about $\epsilon \sim 6\%$ for a non-rotating black hole and $\epsilon \sim 29\%$ for a maximally rotating one (Schneider, 2006).

On the other hand, if the cold matter which was initially at rest and without magnetic field, was subjected to free radial infall it would accrete to the central black hole without any energy release or observational effects (Shakura & Sunyaev, 1973). However, in the case of AGN the accreting matter has a significant angular momentum which does not allow its free infall. At the marginally stable orbit of central black hole with mass of $10^8 M_\odot$, the specific angular momentum is $\approx 1 \times 10^{24}$ cm^2/s, which is much less even in comparison to a typical galaxy where the speciffic angular momentum of orbiting material is $\approx 6 \times 10^{28}$ cm^2/s (Krolik, 1999). It means that approach of accreting material toward a black hole requires a loss of the greatest fraction of its initial angular momentum. Mechanisms which can contribute to such loss of angular momentum are viscosity, nonaxisymmetric gravitational forces, magnetic forces (Krolik, 1999), outflowing winds (Begelman et al., 1983; Elvis, 2000), or the Magnetorotational Instability (MRI) which was discovered by Velikhov (1959) and Chandrasekhar (1960), but did not come to the attention of the astrophysical community until rediscovered by Balbus & Hawley (1991, 1998).

Since the orbit of minimum energy for fixed angular momentum in any spherically symmetric potential is a circle, the infall of accreting material due to loss of its angular momentum will be in form of successively smaller and smaller concentric circles. Matter traveling along orbits inclined to each other will eventually collide in the plane of intersection, and as a result, the angular momenta of different gas steams will be mixed and equalized. Consequently, all accreting matter will orbit in a single plane and will have the same specific angular momentum at any given radius, meaning that accretion is most likely performed through an accretion disk (Krolik, 1999). The assumption of a disk geometry for the distribution of the X-ray emitters in the central parts of AGN is also supported by the spectral shape of the observed Fe Kα line (Nandra et al., 1997, 1999, 2007).

Shakura & Sunyaev (1973) developed what is now called ”standard model of accretion disk”, in which accretion occurs via an optically thick and geometrically thin disk and where the spectrum of thermal radiation emitted from the disk surface depends on its structure and temperature, and therefore on the distance to the central black hole. The distribution of the temperature along the radius of the disk in this model is presented in Fig. 2 (see Popović et al., 2006a, for more details). This model was originally developed to describe the accretion disks around stellar sized black holes in the binary systems, but with certain modifications it could be also applied on accretion disks around central supermassive black holes of AGN.

The total energy release of emitted radiation is mainly determined by the rate of matter inflow into the disk on its outer boundary, i.e. by its accretion rate $\dot{M}$. If the accretion converts matter to radiation with fixed radiative efficiency η (in rest-mass units), then a characteristic scale for the accretion rate is the Eddington accretion rate for which the total release of energy in

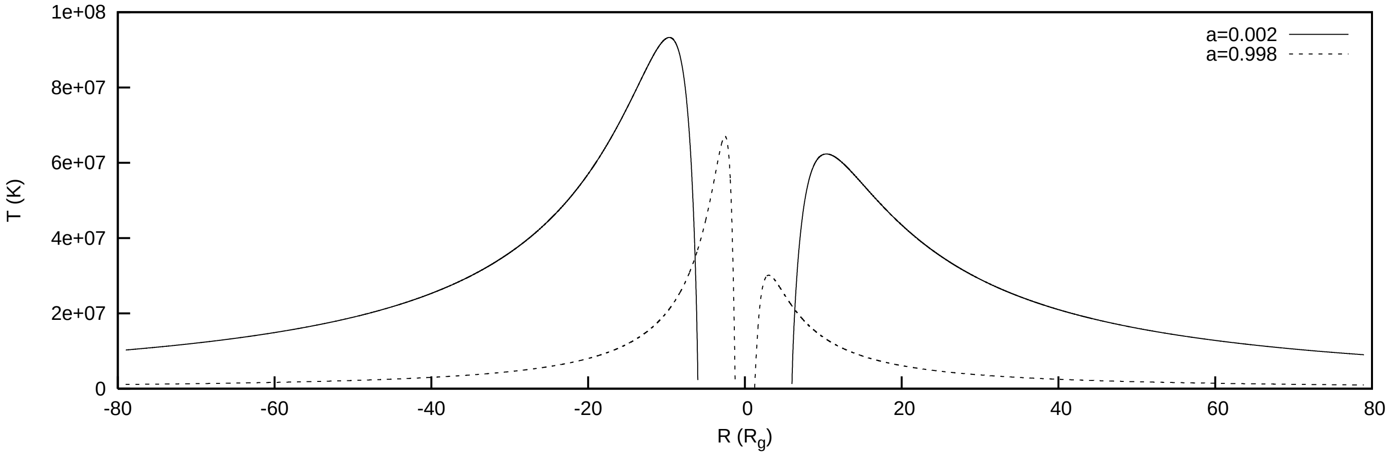

Figure 2: The distribution of the temperature as a function of the disk radius R, given for two different values of angular momentum a. Negative values of R correspond to the approaching and positive values to the receding side of the disk. Image Credit: Popović et al., Copyright: ApJ, 637, 620 (2006).

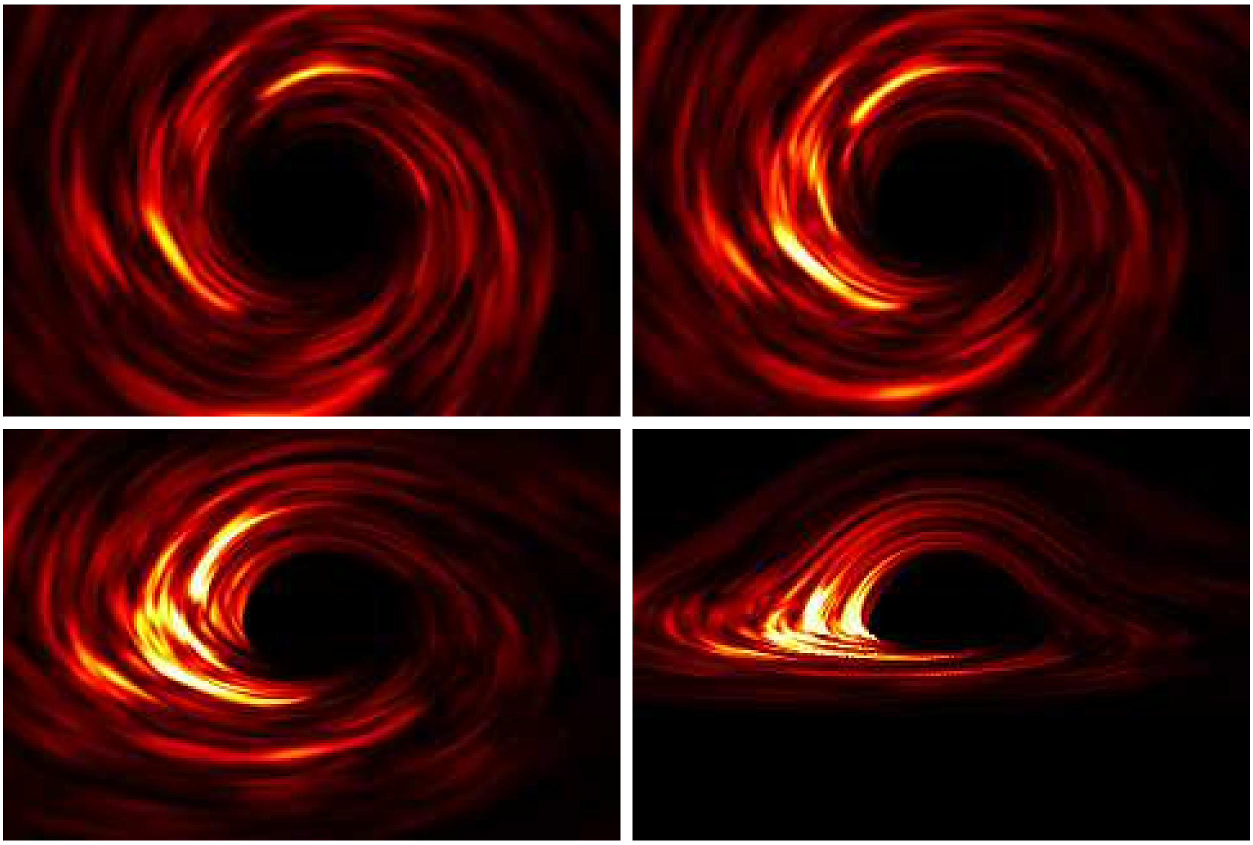

Figure 3: Magnetohydrodynamic simulations of an accretion disk as seen by a distant observer at the following inclination angles (Armitage and Reynolds, 2003): 5° (upper left), 30° (upper right), 55° (lower left) and 80° (lower right). The disk rotation is in counterclockwise direction. Image Credit: Armitage & Reynolds, Copyright: MNRAS, 341, 1041 (2003).

the disk $L = \eta \dot{M} c^2$ is equal to the Eddington luminosity, a critical luminosity beyond which the radiation force overpowers gravity for any given mass (Krolik, 1999; Shakura & Sunyaev, 1973). Observed AGN have luminosities from $\sim 10^{42}$ to $\sim 10^{48}$ erg/s, which means that their central black holes must have masses from 10^5 to 10^9 $M_\odot$ (Krolik, 1999).

Using the Faint Object Spectrograph (FOS) on the Hubble Space Telescope (HST), Harms et al. (1994) found strong evidence for a disk of ionized gas around a supermassive nuclear black hole in M87.

Armitage and Reynolds (2003) performed magnetohydrodynamic simulations of an accretion disk as seen by a distant observer at four different inclinations (see Fig. 3). These simulations showed the existence of especially bright regions in form of arcs within the turbulent flow, which trace out the photon trajectories close to the radius of marginally stable orbit. These arcs are much brighter on approaching side of the disk due to higher surface temperature, as shown in Fig. 3, and also due to Doppler boosting and relativistic beaming which both enhance the flux observed in the direction of motion and diminish the flux in the opposite direction. The influence of these relativistic effects on the shape of the Fe Kα line emitted from the accretion disk will be explained in more details in §2.3.

2. Fe Kα spectral line

2.1. Observational studies

Some observational studies suggest that the broad fluorescent/recombination iron Kα line at 6.4 keV originates from the innermost part of accretion disk, close to the central black hole. For example, using XMM-Newton observation of the broad-line radio galaxy 4C 74.26, Ballantyne & Fabian (2005) found a broad Fe Kα line emitted from a region which had inner radius close to the innermost stable circular orbit (R_{ms}) for a maximally spinning black hole and outer radius within 10 R_g. Therefore, the broad Fe Kα line is an important indicator of accreting flows around supermassive black holes. At the same time, it is the strongest line of the X-ray radiation, and it can be found in the spectra of all types of accreting sources: binary black hole and neutron star systems, cataclysmic variable stars and AGN.

It was first discovered by Mushotzky et al. (1978) in OSO-8 X-ray observations of Cen A (NGC 5128) during 1975 and 1976 (see Fig. 4). NGC 5128 is one of the closest radio galaxies and one of the first extragalactic objects to be identified as an X-ray source. The reflection of the X-rays in K lines of heavy elements from a cold surface was also discussed in the case of the X-ray binaries (see e.g. Basko, 1978), and Exosat Observatory detected a broad emission iron K line at 6.2 keV in the X-ray spectrum of Cyg X-1, a binary X-ray source which was the best known black hole candidate (Barr et al., 1985). Ginga satellite detected a strong iron Kα fluorescence line in a number of Seyfert 1 galaxies (see e.g. Kunieda et al., 1990; Matsuoka et al., 1990; Piro et al., 1990; Pounds et al., 1990; Nandra et al., 1991). The Fe Kα line of active galactic nuclei, as well as different geometries and astrophysical conditions necessary for its emergence, was intensively studied around 1990s (see e.g. Matt et al., 1991; George & Fabian, 1991, and references therein).

The CCD detectors on Japanese *ASCA* satellite were the first instruments with sufficient spectral resolution and sensitivity in the X-ray band, by which Tanaka et al. (1995) obtained the first convincing proof for the existence of a relativistically broadened Fe Kα line in AGN spectra. This discovery was made after four-day observations of Seyfert 1 galaxy MCG-6-30-15 (see Fig. 5).

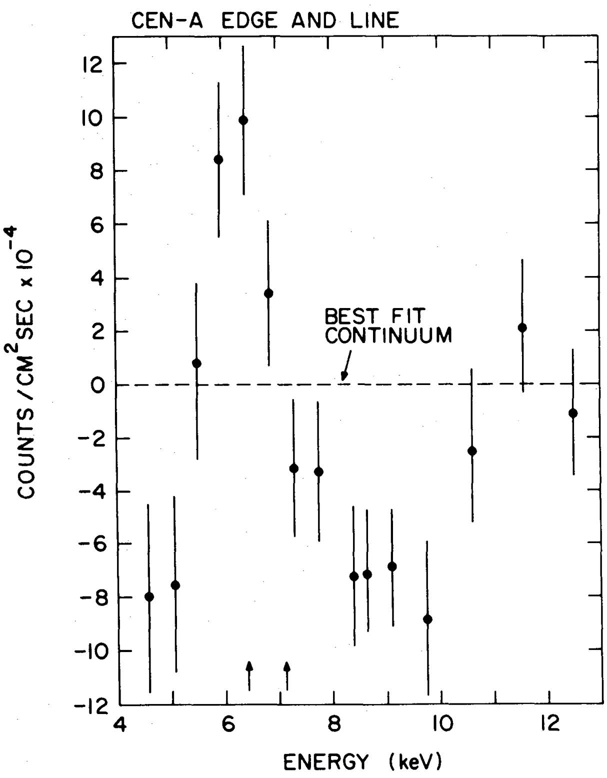

Figure 4: The Fe Kα line of Cen A (NGC 5128) observed by OSO-8 during 1975 and 1976 (Mushotzky et al., 1978). Image Credit: Mushotzky et al., Copyright: ApJ, 220, 790 (1978).

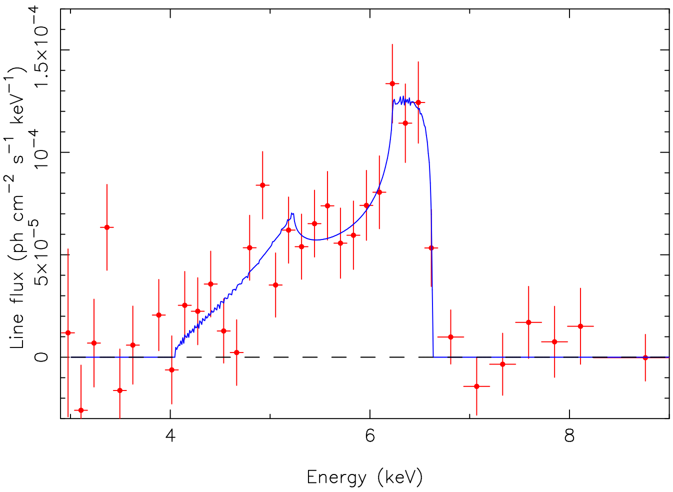

Figure 5: The profile of the Fe Kα line from Seyfert 1 galaxy MCG-6-30-15 observed by *ASCA SIS* detector (Tanaka et al., 1995) and the best fit (blue solid line) obtained by a model of the accretion disk in Schwarzschild metric, extending between 3 and 10 Schwarzschild radii (Fabian et al., 1989). Image Credit: Tanaka et al., Copyright: Nature, 375, 659 (1995). Image generated by Dr. Paul Nandra NASA/GSFC.

Several studies have been performed over samples of local AGN (see e.g. Nandra et al., 1997; Yaqoob et al., 2005; Nandra et al., 2007; Bianchi et al., 2008; Markowitz et al., 2008, etc), as well as from distant quasars (Corral et al., 2008) in order to characterize the Fe Kα emission. Nandra et al. (2007) performed a spectral analysis of a sample of 26 type 1 to 1.9 Seyferts galaxies ($z < 0.05$) observed by *XMM-Newton*. They found that a relativistic line is significantly detected in a half of their sample (54±10%) with a mean equivalent width (EW) of ~ 80 eV, but around 30% of selected AGN showed a relativistic broad line that can be explained by the emission of an accretion disk.

Recent Chandra observations revealed a narrow component of the Fe Kα line in the X-ray spectra of many AGN (see e.g. Yaqoob et al., 2001; Yaqoob & Padmanabhan, 2004; Page et al., 2004; Shu et al., 2010). Although the origin of this narrow component is still poorly understood, it is thought to be produced by emission from material much further from the central black hole, probably in the outermost regions of the accretion disk, in the Broad Line Region (BLR) or torus. Therefore, in the further text the focus will be only on the broad component of the Fe Kα line, which originates from the innermost parts of an relativistic accretion disk.

If the Fe Kα line originated from an arbitrary radius of a non-relativistic (Keplerian) accretion disk it would have a symmetrical profile (due to Doppler effect) with two peaks: a ”blue” one which is produced by emitting material from the approaching side of the disk in respect to an observer, and a ”red” one which corresponds to emitting material from the receding side of the disk. Broadening of the Fe Kα line arises mostly from General Relativistic effects and large rotational velocities of material emitting near the black hole. Using *ASCA* satellite observations, Nandra et al. (1997) found that, in case of 14 Seyfert 1 galaxies, Full-Widths at Half-Maximum (FWHM) of their Fe Kα lines correspond to velocities of $\approx 50,000$ km/s. In some cases (e.g. for Seyfert 1 galaxy MCG-6-30-15), FWHM velocity reaches 30% of speed of light (see e.g. Nandra et al., 2007). It means that in the vicinity of the central black hole, orbital velocities of the emitting material are relativistic, causing the enhancement of the Fe Kα line ”blue” peak in regard to its ”red” peak (relativistic beaming). Taking into account the integral emission in the line over all radii of accretion disk, one can obtain the line with asymmetrical and highly broadened profile (Fabian et al., 2000). The ”blue” peak is then very narrow and bright, while the ”red” one is wider and much fainter (see Fig. 5). Besides, the gravitational redshift causes further deformations of the Fe Kα line profile by smearing the ”blue” emission into ”red” one (see §2.3 for more details). Since the observed Fe Kα line profiles are strongly affected by such relativistic effects, they represent a fundamental tool for investigating the plasma conditions and the space-time geometry in the vicinity of the supermassive black holes of AGN.

2.2. Production of the Fe Kα line

A substantial amount of X-ray radiation of AGN is thought to be emitted from the hot corona sandwiching the accretion disk (see Fig. 6). The Fe Kα line is produced when the hot corona irradiates the relatively cold accretion disk by the hard X-ray power law continuum, causing among the rest, photoelectric absorption followed by fluorescent line emission (Fabian et al., 2000). When plasma is subjected to the influence of the hard X-ray radiation, one of the two K-shell ($n = 1$, where n is the principal quantum number) electrons of an iron atom (or ion) is ejected following the photoelectric absorption of an X-ray (Fabian et al., 2000). The threshold for the absorption by neutral iron is 7.1 keV (Fabian et al., 2000). The resulting excited state decays when an L-shell ($n = 2$) electron drops into the K-shell, releasing 6.4 keV of energy. This energy is either emitted as an emission-line photon (34% probability) or internally absorbed by another electron (66% probability) which is consequently ejected from the iron ion (Auger effect).

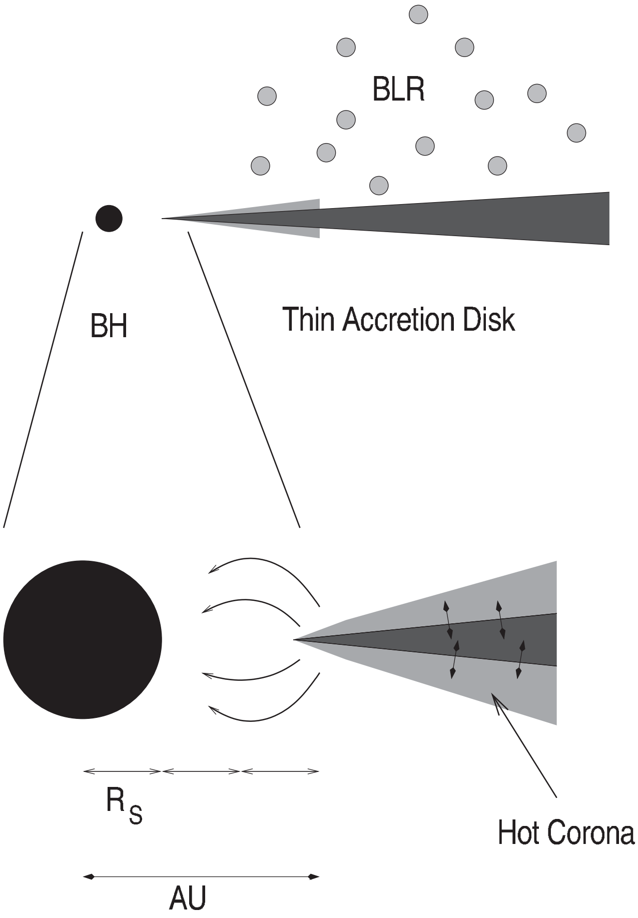

Figure 6: Schematic illustration of inner region of accretion disk around black hole, where the Fe Kα line is produced. Image Credit: Wilms et al., Copyright: MemSAI, 75, 519 (2004).

The fluorescent yield (i.e. the probability that photoelectric absorption is followed by fluorescent line emission rather than the Auger effect) is a weak function of the ionization state from neutral iron (Fe I) up to Fe XXIII (Fabian et al., 2000). For lithium-like iron (Fe XXIV) through to hydrogen-like iron (Fe XXVI), the lack of at least two electrons in the L-shell means that the Auger effect cannot occur. For He and H-like iron ions, the line is produced by the capture of free electrons (recombination) and the equivalent fluorescent yield is high and it depends on the plasma conditions (Fabian et al., 2000).

For the neutral iron, the Fe Kα line energy is 6.4 keV (more precisely, there are two components of the line (Fabian et al., 2000): Fe Kα_1 at 6.404 and Fe Kα_2 at 6.391 keV), while in the case of ionization, the energy of both the photoelectric threshold and the Fe Kα line are slightly increased. Even for such high ionization states of He and H-like iron ions, the Fe Kα line energy is increased only to 6.7 and 6.9 keV, respectively (Krolik, 1999). Importance of ionization, X-ray scattering and

Compton reflection on the properties of the observed Fe Kα line, was discussed by Turner et al. (1997), based upon the analysis of *ASCA* observations of 25 Seyfert 2 galaxies.

Fe Kα line is pretty narrow in itself, but in case when it originates from a relativistically rotating accretion disk of AGN it becomes wider due to kinematic effects, and also its shape (or profile) is changed due to Doppler boosting and gravitational redshift (see Fig. 7). Such broadening of the line is very often observed in spectra of Seyfert galaxies and is one of the main evidences for the existence of a relativistic accretion disk which extends deeply in the gravitational field of the central black hole (Życki, 2004).

2.3. Theoretical studies

In general, there are several approaches to numerically evaluate the line profiles emitted by the accretion disk around black hole (Reynolds & Nowak, 2003): i) analytically in the weak field limit (Chen et al., 1989; Chen & Halpern, 1989) and in the Schwarzschild metric (Fabian et al., 1989; Stella, 1990; Matt et al., 1992), ii) by brute-force using the direct integration of the photon trajectory in the Kerr metric (e.g. Karas et al., 1992), iii) by expressing observed flux over transfer-function containing all relativistic effects (Cunningham, 1975), and iv) using so called ray-tracing method in Kerr metric (Bao et al., 1994; Bromley et al., 1997; Fanton et al., 1997; Čadež et al., 1998).

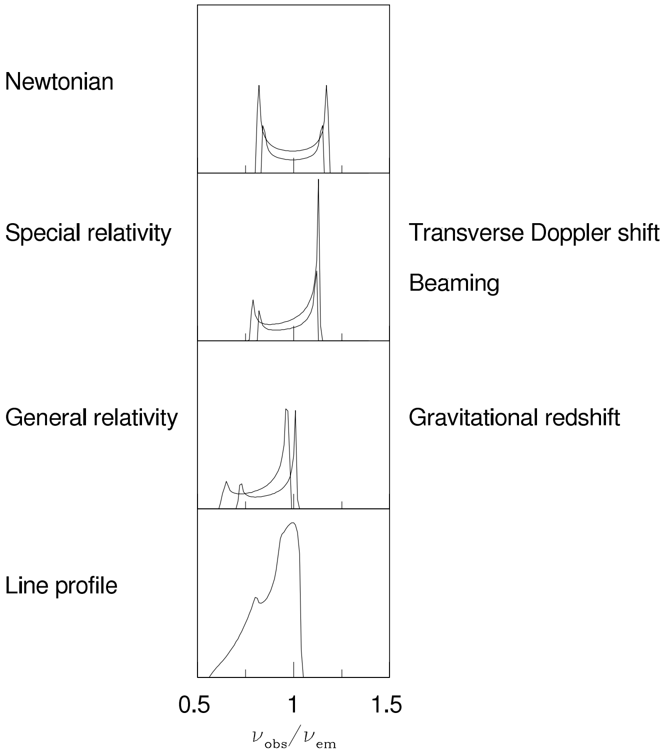

Figure 7: The influence of Doppler and transverse-Doppler shifts, relativistic beaming and gravitational redshifting on profile of the Fe Kα line emitted by an accretion disk around a black hole. Image Credit: Fabian et al., Copyright: PASP, 112, 1145 (2000).

Chen et al. (1989) and Chen & Halpern (1989) developed an approach for calculating the intensities and profiles of the lines emitted from a Keplerian accretion disk in which the relativistic effects are included in the weak-field limit. Rigorous relativistic calculations of the Fe Kα line profile emitted from a geometrically thin accretion disk around a stationary black hole, i.e. in the case of Schwarzschild metric have been carried out by e.g. Fabian et al. (1989); Stella (1990); Matt et al. (1992). The relativistic effects on the continuum emission from an accretion disk around a rotating black hole (i.e. for Kerr metric) were first calculated by Cunningham (1975), while the line profiles in such a case were simulated by Laor (1991). Fabian et al. (2000) studied the influence of Doppler effect and gravitational redshift on the shape of Fe Kα line emitted by an accretion disk around a black hole and found that, as a result, the line profile appears to be broadened and skewed (see Fig. 7).

The emission from accretion disk can be analyzed also by numerical simulations based on ray-tracing method in Kerr metric (Bao et al., 1994; Bromley et al., 1997; Fanton et al., 1997; Čadež et al., 1998), taking into account only photon trajectories reaching the observer's sky plane. In this method one divides the image of the disk on the observer's sky into a number of small elements (pixels). For each pixel, the photon trajectory is traced backward from the observer by following the geodesics in a Kerr space-time, until it crosses the plane of the disk (see Fig. 8). Then, the flux density of the radiation emitted by the disk at that point, as well as the redshift factor of the photon are calculated. In that way, one can obtain the color images of the accretion disk which a distant observer would see by a high resolution telescope. The simulated line profiles can be calculated taking into account the intensities and received photon energies of all pixels of the corresponding disk image. Čadež et al. (1998) developed a variant of ray-tracing method based on the pseudo-analytical integration of the geodesic equations which describe the photon trajectories in the Kerr metric.

The complex profile of the Fe Kα line depends on different parameters of the accretion disk and central black hole (see e.g. Fabian et al., 2000). In order to study the size of the Fe Kα line emitting region, as well as its location in the disk, one can assume that the line is emitted from a region in form of a narrow ring. For example, Jovanović & Popović (2008) assumed a line emitting region with width equals to 1 R_g, located between: a) R_{in} = 6 R_g and R_{out} = 7 R_g and b) R_{in} = 50 R_g and R_{out} = 51 R_g. These two cases are presented in Fig. 9. From Fig. 9 one can see how the Fe Kα line profile is changing as the function of distance from central black hole. When the line emitters are located at the lower radii of the disk, i.e. closer to the central black hole, they rotate faster and the line is broader and more asymmetric (see Fig. 9 top-right). If the line emission is originating at larger distances from the black hole, its emitting material is rotating slower and therefore the line becomes narrower and more symmetric (see Fig. 9 bottom-right). In majority of AGN, where the broad Fe Kα line is observed, its profile is more similar to the modeled profile as obtained under assumption that the line emitters are located close to the central black hole (Tanaka et al., 1995; Nandra et al., 2007; Jovanović & Popović, 2008).

Angular momentum or spin of the central supermassive black hole of AGN is a property of the space-time metric and dif-

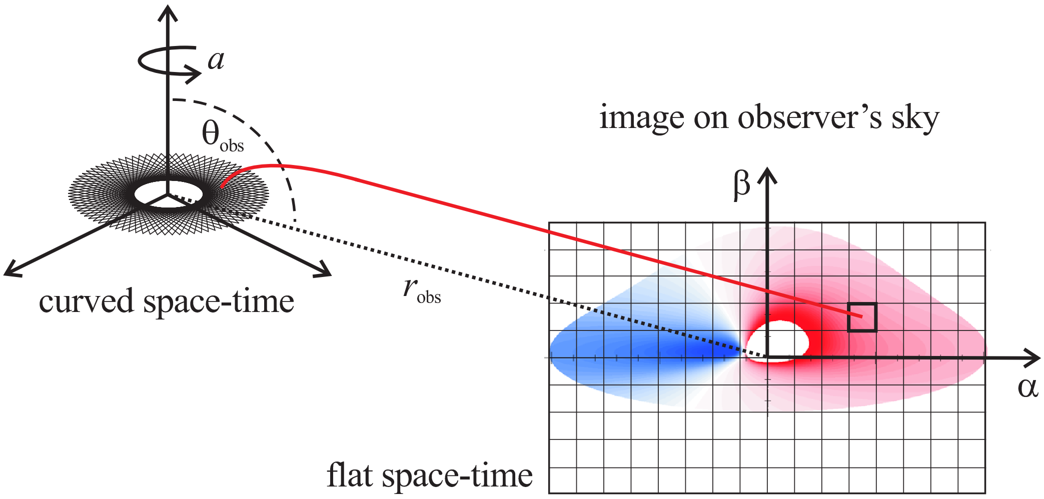

Figure 8: Schematic illustration of the ray-tracing method in the Kerr metric, showing a light ray emitted from some radius of accretion disk in coordinate system defined by a rotating black hole with angular momentum a, and observed at a pixel with coordinates (impact parameters) α, β on the disk image in the observer's reference frame. Image Credit: Jovanović & Popović, Copyright: Black Holes and Galaxy Formation, Nova Science Publishers Inc, Hauppauge NY, USA, 249-294 (2009).

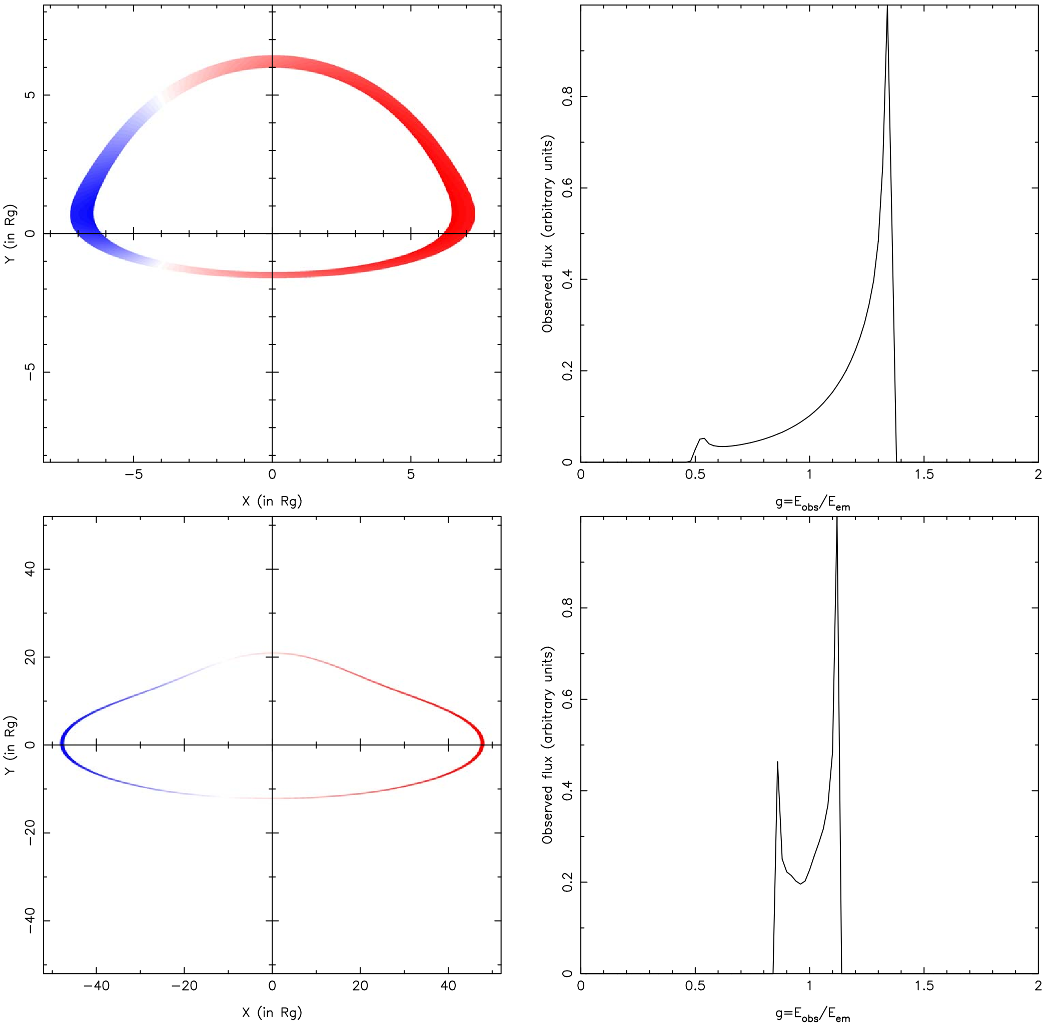

Figure 9: *Left:* illustrations of the Fe Kα line emitting region in form of narrow ring with width = $1R_g$, extending from: R_{in} = 6 R$_g$ to R_{out} = 7 R$_g$ (top) and R_{in} = 50 R$_g$ to R_{out} = 51 R$_g$ (bottom). *Right:* the corresponding Fe Kα line profiles. Image Credit: Jovanović & Popović, Copyright: Fortschr. Phys., 56, 456 (2008).

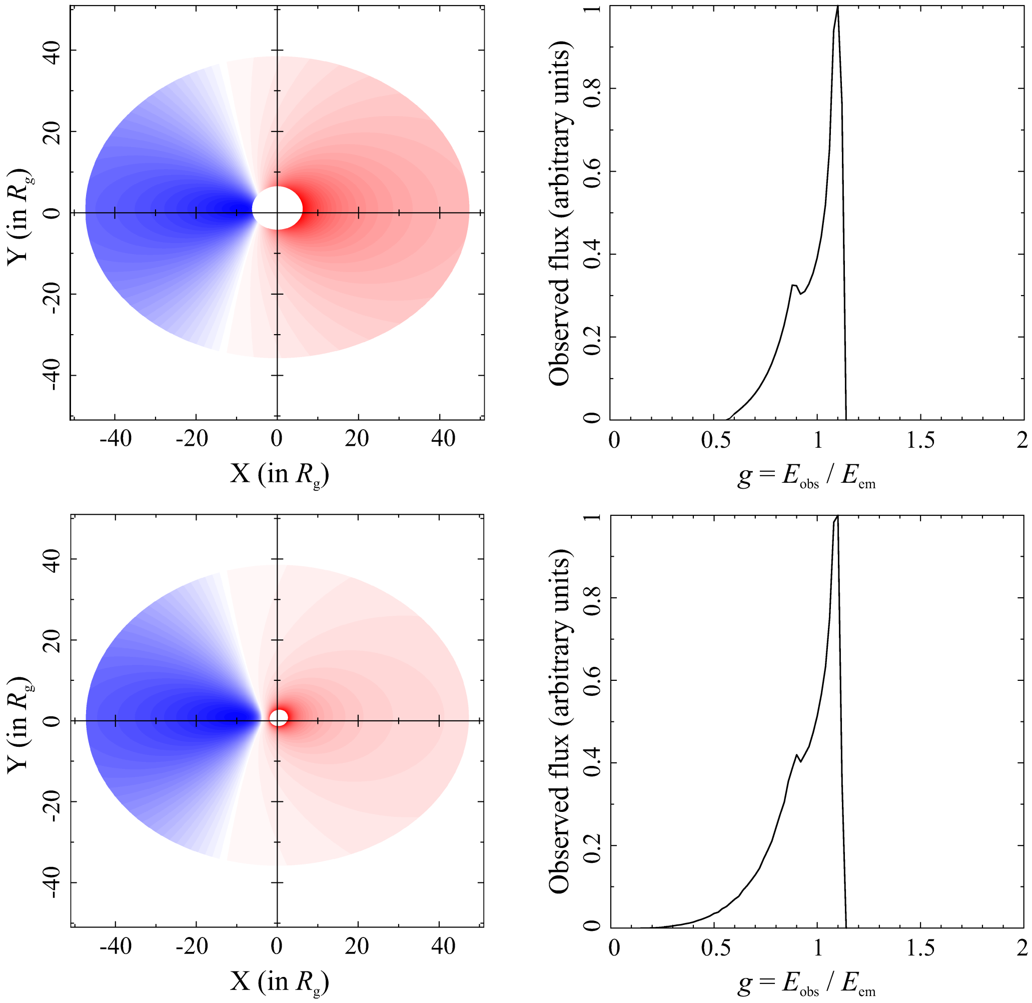

Figure 10: Illustrations of an accretion disk (left panels) and the corresponding Fe Kα line profiles (right panels) for disk inclination $i = 40°$ in the Kerr metric for angular momentum $a = 0.1$ (*top*) and $a = 0.998$ (*bottom*). Image Credit: Jovanović et al., Copyright: Baltic Astronomy (2011).

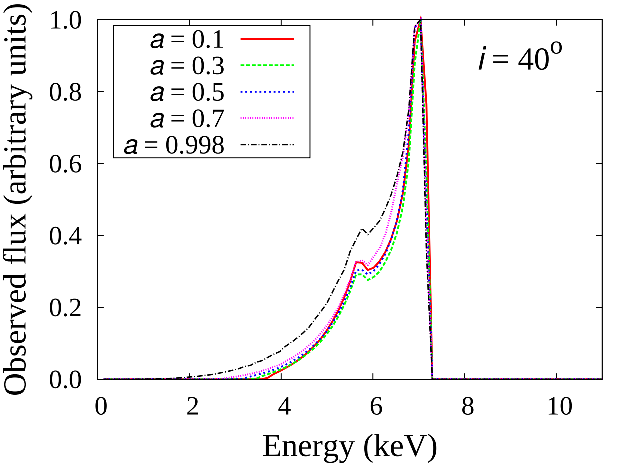

Figure 11: Modeled Fe Kα spectral line profiles for several values of angular momentum parameters a, and for inclination angle $i = 40°$. Image Credit: Jovanović et al., Copyright: Baltic Astronomy (2011).

ferent techniques for its estimation are developed (see e.g. Czerny et al., 2011; Daly, 2011). To study the effects of black hole spin on the shape of the Fe Kα line we performed simulations of disk emission based on ray-tracing method in Kerr metric. Simulated images of an accretion disk around a supermassive black hole and the corresponding Fe Kα line profiles for two different values of its spin are presented in Fig. 10 (see Jovanović et al., 2011, for more details). In these simulations, the disk extends from the radius of marginally stable orbit (R_{ms}) to 40 R_g, where R_g is the gravitational radius. As one can see from Fig. 10, R_{ms} strongly depends on black hole spin, which consequently also affects the profile of the line originating in the innermost parts of the disk (see also Brenneman & Reynolds, 2006). Simulated Fe Kα line profiles for several values of black hole spin are presented in Fig. 11 (Jovanović et al., 2011). It can be seen from Fig. 11 that the black hole spin especially affects the red wing of the Fe Kα line, and that this wing is more extended towards lower energies for higher values of the spin (see Reynolds & Nowak, 2003; Jovanović & Popović, 2008; Jovanović et al., 2011). At the same time, the line becomes wider and its red peak brighter.

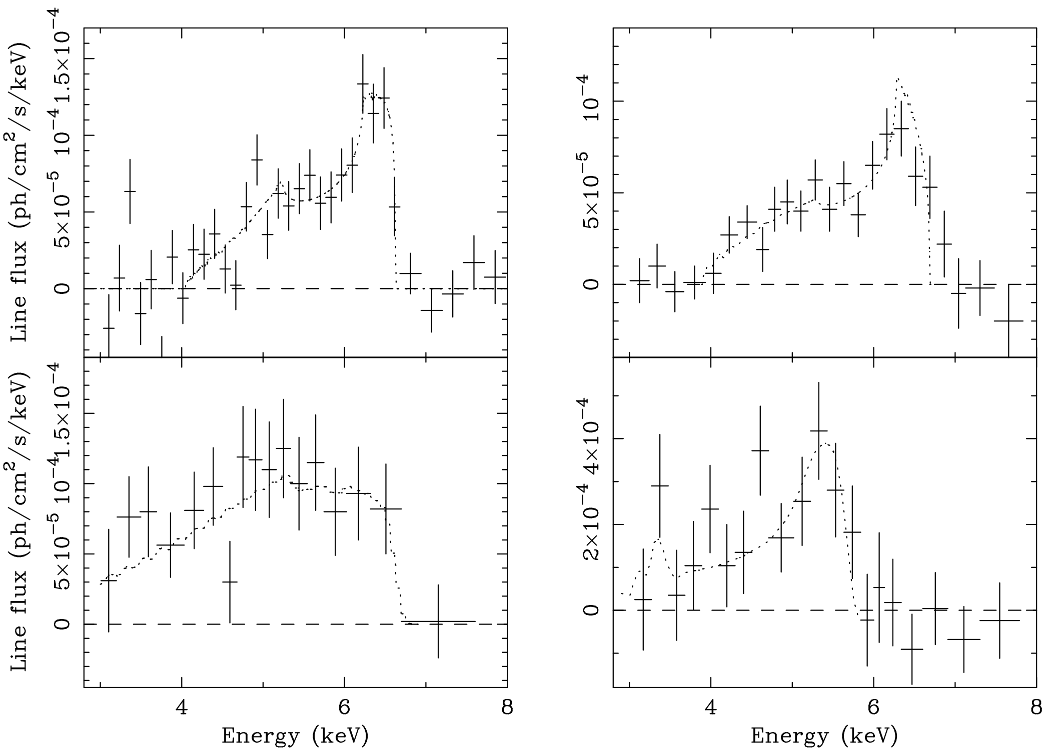

Figure 12: Time-averaged (upper panels) and peculiar line profiles (lower panels) of the Fe Kα line in the case of MCG –6-30-15 observed by *ASCA* in 1994 (left panels) and 1997 (right panels). Image Credit: Fabian et al., Copyright: PASP, 112, 1145 (2000).

2.4. Variability of the Fe Kα line

One of the important features of the Fe Kα line is variability of both, its shape and intensity (see e.g. Bhayani & Nandra, 2010, and references therein). Fig. 12 shows one of the most illustrative examples for such variations which was found in *ASCA* observations of MCG–6-30-15 during 1994 and 1997 (Fabian et al., 2000). As it can be seen from Fig. 12, in the 1994 observation, a very broad profile with a pronounced red wing is seen during a period of deep minimum of the light curve (lower left panel), compared to the time-averaged line profile shown in the upper panel. In contrast, during a sharp flare in the 1997 observation, the whole line emission is shifted to energies below 6 keV, and there is no significant emission at the rest line energy of 6.4 keV (lower right panel). Both peculiar line shapes can be explained by large gravitational redshift in small radii on the accretion disk Fabian et al. (2000).

Variations of double-peaked emission lines are mainly attributed to physical changes in the accretion disk, but in case of some AGN they cannot be explained by a simple, circular accretion disk model, and thus the need for asymmetries in the accretion disk arose. Such asymmetries are usually introduced in form of a precessing elliptical disk (Eracleous et al., 1995), a circular disk with a spiral arms (Lewis et al., 2010) or with rotating bright spots (Flohic & Eracleous, 2008).

Iwasawa et al. (2004) detected a variable ”red” feature of the Fe Kα line at 6.1 keV (in addition to the stable 6.4 keV line core) in X-ray spectrum of Seyfert galaxy NGC 3516, observed by *XMM-Newton* satellite (see Fig. 13). This feature varies systematically in the flux at intervals of 25 ks and in energy

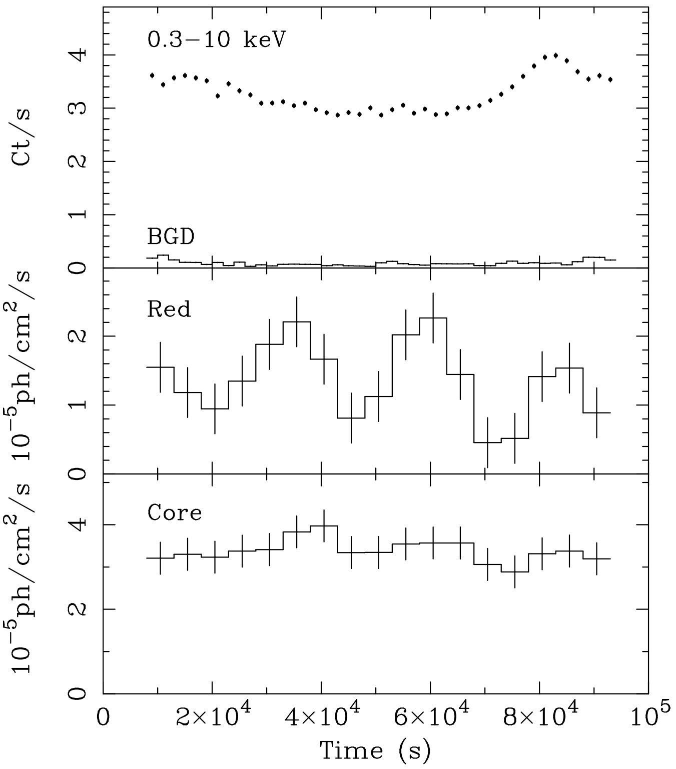

Figure 13: Light curves of Seyfert galaxy NGC 3516 (Iwasawa et al., 2004) for: the 0.3 – 10 keV band (top), the Fe Kα line red feature (middle) and the 6.4 keV line core (bottom). Image Credit: Iwasawa et al., Copyright: MNRAS, 355, 1073 (2004).

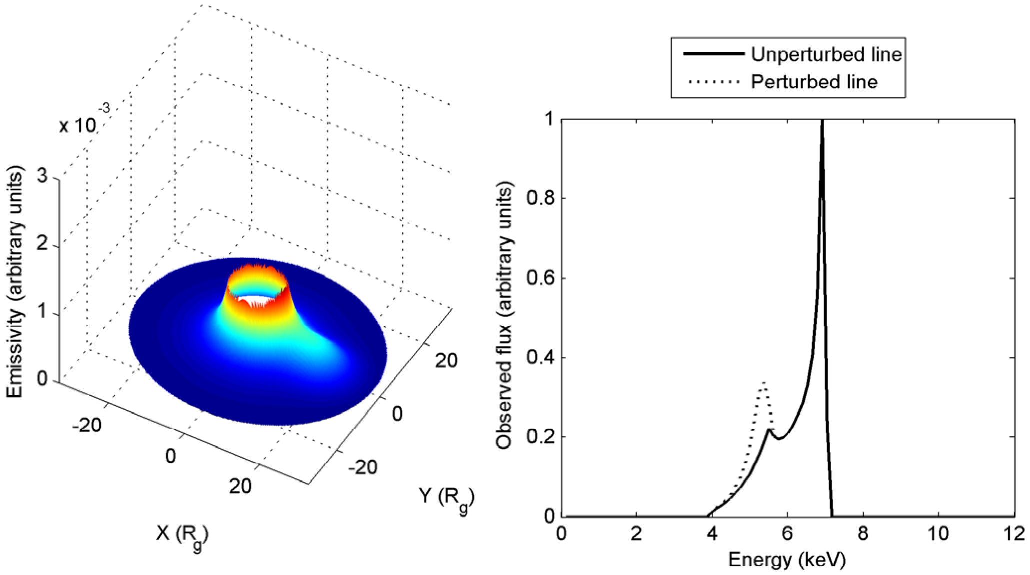

Figure 14: *Left:* perturbed emissivity of an accretion disk in Schwarzschild metric (Jovanović & Popović, 2009). *Right:* the corresponding perturbed (dashed line) and unperturbed (solid line) Fe Kα line profiles. Image Credit: Jovanović & Popović, Copyright: Black Holes and Galaxy Formation, Nova Science Publishers Inc, Hauppauge NY, USA, 249-294 (2009).

between 5.7 and 6.5 keV. Iwasawa et al. (2004) found that the spectral evolution of the ”red” feature agrees well with hypothesis of an orbiting spot in the accretion disk.

Appearances of such bright spots could be described by perturbations in accretion disk emissivity (Jovanović et al., 2010) and could be caused by several physical mechanisms, such as: disk self-gravity, baroclinic vorticity, disk-star collisions, tidal disruptions of stars by central black hole and fragmented spiral arms of the disk (see e.g. Jovanović et al., 2010, and references therein). All these phenomena have different occurrence frequencies, durations, timescales, strengths, proportions and other characteristics. Especially, perturbations of accretion disk emissivity in form of flares with high amplitudes are of great significance because they could provide information on accretion physics under extreme conditions. Such flares with the highest amplitudes are usually interpreted in terms of tidal disruptions of stars by supermassive black holes (see e.g. Komossa et al., 2008, and references therein). Stars approaching a SMBH will be tidally disrupted once the tidal forces of the SMBH exceed the star's self-gravity, and part of the stellar debris will be accreted, producing a luminous flare of radiation which lasts on the timescale of months to years. Although, frequency of such events in a typical elliptical galaxy is very low, between 10^{-5} and 10^{-4} per year (see e.g. Jovanović et al., 2010, and references therein), recently Komossa et al. (2008) reported the discovery of an X-ray outburst of large amplitude in the galaxy SDSS J095209.56+214313.3 which was probably caused by the tidal disruption of a star by a supermassive black hole. A simulation of such perturbed emissivity of an accretion disk in Schwarzschild metric, as well as the corresponding perturbed and unperturbed Fe Kα line profiles, are presented in the left and right panels of Fig. 14, respectively (Jovanović & Popović, 2009).

Most AGN contain energetic outows of ionized gas, emerging from their accretion disks at relativistic speeds, which imprint multiple broad absorption features blueward of the emission lines (see e.g. Chartas et al., 2002b). These additional absorption components, arising from outflowing winds, may distort the energy region near the Fe Kα line. Recently, Chartas et al. (2009) confirmed the presence of X-ray broad absorption lines from the quasar APM 08279+5255, varying on short timescales of several days which implies a source size-scale of $\sim$ 10 R_g (see also Brandt et al., 2009). Done et al. (2007) found an evidence for a P Cygni profile of the Fe Kα line in narrow line Seyfert 1 galaxies and showed that a sharp drop in a such profile at $\sim$ 7 keV results from absorption/scattering/emission of the iron Kα line in the outflowing wind.

In addition to intrinsic causes such as a disk instability, the Fe Kα line variability could also be induced by some external effects, such as absorption by X-ray absorbers or gravitational microlensing (Jovanović & Popović, 2009). Observations of so-called Low Ionization Broad Absorption Line quasars (e.g. Mrk 231 Braito et al., 2004) and (H 1413+117 Chartas et al., 2007) confirmed the presence of X-ray absorbers in these objects. Wang et al. (2001) detected an absorption line at 5.8 keV in nearby Seyfert 1.5 galaxy NGC 4151 and a variable absorption line at the same energy has been discovered by Nandra et al. (1999) in NGC 3516. It was interpreted as a Fe K resonant absorption line, redshifted either by infalling absorbing material or by strong gravity in the vicinity of the black hole. A model of the Fe Kα line absorbing/obscuring regions in form of absorbing medium comprised of cold absorbing cloudlets was developed by Fuerst & Wu (2004). Another model, which assumes that absorbing region is composed of a number of individual spherical absorbing clouds, was developed by Jovanović & Popović (2007).

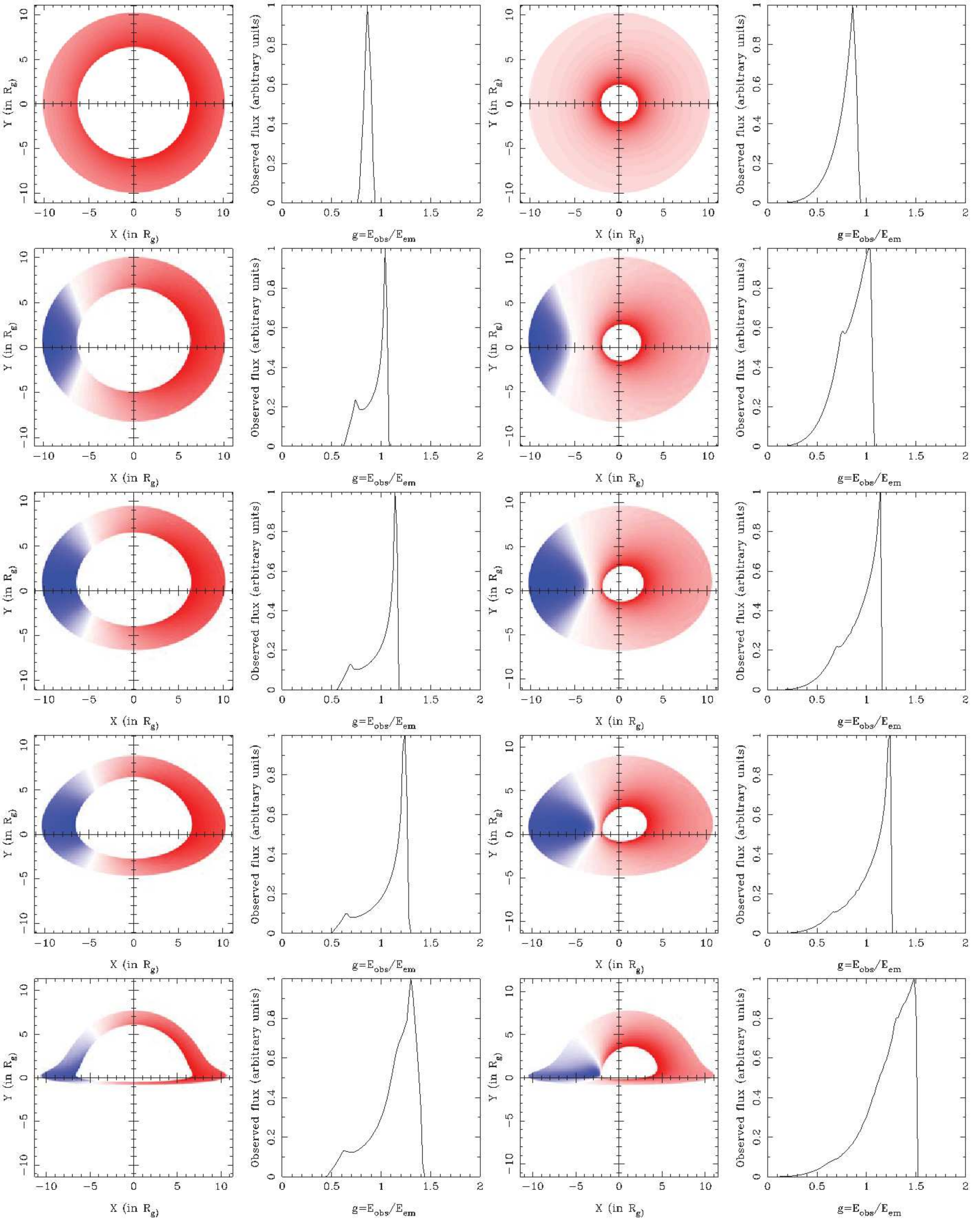

Figure 15: *Left:* Simulated images of accretion disk in Schwarzschild metric and the corresponding Fe Kα line profiles. *Right:* The same, but in Kerr metric for maximally rotating black hole, i.e. for $a = 0.998$. Disk inclination takes the following values from top to bottom panels, respectively: $i = 5°$, $30°$, $45°$, $60°$, $85°$.

Popović et al. (2001) found that a compact gravitational microlens could induce noticeable changes in the Fe Kα line profile when the Einstein ring radius associated with the microlens is comparable to the size of the accretion disk. Also, the X-ray continuum could experience significant amplification during such microlensing events (Popović et al., 2006b). Zakharov et al. (2004) found that cosmologically distributed gravitational microlenses could significantly contribute to the X-ray variability of high-redshifted ($z > 2$) quasars. Indeed, microlensing of the Fe Kα line has been reported at least in three lensed quasars with multiple images: MG J0414+0534 (Chartas et al., 2002a), QSO 2237+0305 (Dai et al., 2003), and H 1413+117 (Oshima et al., 2001; Chartas et al., 2004). Chartas et al. (2002a) detected an increase of the Fe Kα equivalent width in the image B of MG J0414+0534 which was not followed by the continuum and explained this behavior by assumption that the thermal emission region of the disk and the Compton up-scattered emission region of the hard X-ray source lie within smaller radii than the iron-line reprocessing region. Dai et al. (2003) also measured amplification of the Fe Kα line in component A of QSO 2237+0305. For more detailed discussion about observational and theoretical investigations of the Fe Kα line variability due to gravitational microlensing see e.g. Jovanović (2005, 2006); Jovanović et al. (2008) and Popović et al. (2003a,b); Popović et al. (2006a), as well as references therein.

3. Discussion

In order to demonstrate the consequences on the Fe Kα line of some general relativistic and strong gravitational effects, which are significant only near the marginally stable orbit, we performed ray-tracing simulations (using approach proposed by Čadež et al., 1998) of a disk emission from its innermost regions. For that purpose we analyzed several cases for disk inclination and spin, assuming that the disk extends from the R_{ms} to 10 R_g, which is the region where the line is most likely produced in most AGN (see e.g Ballantyne & Fabian, 2005).

The obtained results are presented in Fig. 15. As one can see from the Fig. 15, for all studied inclinations there are significant differences between the simulated line profiles in the case of non-rotating and maximally rotating black hole. In the latter case the line profiles are generally wider and more extended towards lower observed energies (see also Fig. 11), due to fact that the disk extends from the radius of marginally stable orbit, which is much smaller in this case (Jovanović et al., 2011). This effect, when observed, gives opportunity to measure black hole spin, and thus to have insight into space-time geometry in its vicinity. At the same time, as a consequence of gravitational redshift, the ”blue” peak is more smeared than the ”red” one in the case of maximally rotating black hole. Therefore, comparisons between the observed and simulated Fe Kα line profiles enables us to investigate the effects of strong gravitational field predicted by General Relativity. However, since the spectrum ”reflected” from the disk may contain not only a single iron line, but also many fluorescent lines and a continuum reflection component (see e.g. Fabian, 2006), accurate modeling of the underlying reflected and direct components is crucial in using the Fe Kα line as a diagnostic of General Relativity in the strong field regime.

Except the black hole spin, the disk inclination also have significant influence on the line profile, as can be seen from Fig. 15. For small inclinations, i.e. in the case of almost face-on disk, the single peak profiles of the Fe Kα line are obtained. For inclinations about $i \approx 30^\circ$, the faint ”red” peak is the most emphasized. It is interesting that this value is close to the averaged value of $i = 35^\circ$, estimated by Nandra et al. (1997) from the study of the Fe Kα line profiles of 18 Seyfert 1 galaxies.

4. Conclusions

The results of previously mentioned observational and theoretical studies indicate that the broad Fe Kα line which originates in vicinity of the supermassive black holes is a powerful tool for studying their properties, space-time geometry (metric) in their vicinity, their accretion physics, probing the effects of their strong gravitational fields, and for testing the certain predictions of General Relativity. However, some important scientific issues still need to be addressed, such as decoupling the narrow and broad Fe Kα line components and explaining their different variabilities (see e.g Sulentic et al., 1998). This will be one of the crucial steps in determining the real importance of relativistic effects on the observed Fe Kα line profiles.

Acknowledgements. This work is part of the project 176003 ”Gravitation and the Large Scale Structure of the Universe“ supported by Ministry of Education and Science of the Republic of Serbia. It was presented as an invited talk at special workshop ”Spectral lines and super-massive black holes” held on June 10, 2011 as a part of activity in the frame of COST action 0905 ”Black holes in a violent universe”, during the ”8th Serbian Conference on Spectral Line Shapes in Astrophysics”.

References

Antonucci, R. 1993, ARA&A, 31, 473
Armitage, P. J., Reynolds, C. S. 2003, MNRAS, 341, 1041
Balbus, S. A., & Hawley, J. F. 1991, ApJ, 376, 214
Balbus, S. A., & Hawley, J. F. 1998, Reviews of Modern Physics, 70, 1
Ballantyne, D. R., & Fabian, A. C. 2005, ApJ, 622, L97
Bao, G., Hadrava, P., Ostgaard, E. 1994, ApJ, 435, 55
Bardeen, J. M. 1970, Nature, 226, 64
Barr, P., White, N. E., & Page, C. G. 1985, MNRAS, 216, 65
Basko, M. M. 1978, ApJ, 223, 268
Begelman, M. C., McKee, C. F., & Shields, G. A. 1983, ApJ, 271, 70
Bhayani, S., & Nandra, K. 2010, arXiv:1006.1982
Bianchi, S., La Franca, F., Matt, G. et al. 2008, MNRAS, 389L, 52
Boyer, R. H., & Lindquist, R. W. 1967, Journal of Mathematical Physics, 8, 265
Braito, V., Della Ceca, R., Piconcelli, E., Severgnini, P., Bassani, L., Cappi, M., Franceschini, A., Iwasawa, K., Malaguti, G., Marziani, P., Palumbo, G. G. C., Persic, M., Risaliti, G., Salvati, M. 2004, A&A, 420, 79
Brandt, W. N., Chartas, G., Gallagher, S. C., Gibson, R. R., & Miller, B. P. 2009, American Institute of Physics Conference Series, 1201, 49
Brenneman, L. W., Reynolds, C. S. 2006, ApJ, 652, 1028
Bromley, B.C., Chen, K., Miller, W.A. 1997, ApJ, 475, 57
Čadež, A., Fanton, C., Calivani, M. 1998, New A, 3, 647
Carter, B. 1968, Physical Review, 174, 1559

Carter, B. 1973, in Black Holes (Les Houches 1972), Eds. De Witt, C. and De Witt, B. S., Gordon and Breach, New York, pp. 57-214
Chandrasekhar, S. 1931, ApJ, 74, 81
Chandrasekhar, S. 1960, Proc. Natl. Acad. Sci. USA, 46, 253
Chandrasekhar, S. 1983, The mathematical theory of black holes, International Series of Monographs on Physics, Volume 69, Oxford University Press, New York
Chartas, G., Agol, E., Eracleous, M., Garmire, G., Bautz, M. W., Morgan, N. D. 2002, ApJ, 568, 509
Chartas, G., Brandt, W. N., Gallagher, S. C., & Garmire, G. P. 2002, ApJ, 579, 169
Chartas, G., Eracleous, M., Agol, E., Gallagher, S. C. 2004, ApJ, 606, 78
Chartas, G., Eracleous, M., Dai, X., Agol, E., Gallagher, S. 2007, ApJ, 661, 678
Chartas, G., Saez, C., Brandt, W. N., Giustini, M., & Garmire, G. P. 2009, ApJ, 706, 644
Chen, K., & Halpern, J. P. 1989, ApJ, 344, 115
Chen, K., Halpern, J. P., & Filippenko, A. V. 1989, ApJ, 339, 742
Corral, A., Page, M.J., Carrera, F.J., Barcons, X. Mateos, S., Ebrero, J., Krumpe, M., Schwope, A., Tedds, J.A., Watson, M.G. 2008, A&A, 492, 71
Cunningham, C. T., & Bardeen, J. M. 1972, ApJ, 173, L137
Cunningham, C. T., & Bardeen, J. M. 1973, ApJ, 183, 237
Cunningham, C. T. 1975, ApJ, 202, 788
Czerny, B., Hryniewicz, K., Nikołajuk, M., & Sądowski, A. 2011, MNRAS, 415, 2942
Dai, X., Chartas, G., Agol, E., Bautz, M. W., Garmire, G.P. 2003, ApJ, 589, 100
Daly, R. A. 2011, MNRAS, 414, 1253
Done, C., Sobolewska, M. A., Gierliński, M., Schurch, N. J. 2007, MNRAS, 374, L15
Einstein, A. 1916, Annalen der Physik, 49, 769
Elvis, M. 2000, ApJ, 545, 63
Eracleous, M., Livio, M., Halpern, J. P., & Storchi-Bergmann, T. 1995, ApJ, 438, 610
Fabian, A. C., Rees, M. J., Stella, L., & White, N. E. 1989, MNRAS, 238, 729
Fabian, A. C., Iwasawa, K., Reynolds, C. S., & Young, A. J. 2000, PASP, 112, 1145
Fabian, A. C. 2006, Proceedings of The X-ray Universe 2005 (ESA SP-604), 604, 463
Fanton, C., Calivani, M., Felice, F., Čadež, A. 1997, PASJ, 49, 159
Ferrarese, L., & Ford, H. 2005, Space Sci. Rev., 116, 523
Flohic, H. M. L. G., & Eracleous, M. 2008, ApJ, 686, 138
Fuerst, S. V., Wu, K. 2004, A&A, 424, 733
George, I. M., & Fabian, A. C. 1991, MNRAS, 249, 352
Harms, R. J., et al. 1994, ApJ, 435, L35
Hewish, A., Bell, S. J., Pilkington, J. D. H., Scott, P. F., & Collins, R. A. 1968, Nature, 217, 709
Iwasawa, K., Miniutti, G., Fabian, A.C. 2004, MNRAS, 355, 1073
Jovanović, P. 2005, Mem. Soc. Astron. Italiana, 7, 56
Jovanović, P. 2006, PASP, 118, 656
Jovanović, P., Popović, L. Č. 2007, AIP Conf. Proc., 938, 76
Jovanović P., Popović L. Č. 2008, Fortschritte der Physik, 56, 456
Jovanović, P., Zakharov, A.F., Popović, L.Č., Petrović, T. 2008, MNRAS, 386, 397
Jovanović P., Popović L. Č. 2009, chapter in the book Black Holes and Galaxy Formation, Nova Science Publishers Inc, Hauppauge NY, USA, 249-294 (arXiv:0903.0978)
Jovanović, P., Popović, L. Č., Stalevski, M., Shapovalova, A. I. 2010, ApJ, 718, 168
Jovanović, P., Borka Jovanović, V., Borka, D. 2011, Baltic Astronomy, 20, 468
Karas, V., Vokrouhlicky, D., & Polnarev, A. G. 1992, MNRAS, 259, 569
Kaspi, S., Smith, P. S., Netzer, H., Maoz, D., Jannuzi, B. T., Giveon, U. 2000, ApJ, 533, 631
Kerr, R. P. 1963, Physical Review Letters, 11, 237
Komossa, S., et al. 2008, ApJ, 678, L13
Krolik, J. H. 1999, Active galactic nuclei : from the central black hole to the galactic environment, Princeton University Press, Princeton, New Jersey
Kunieda, H., Awaki, H., Koyama, K., Turner, T. J., & Mushotzky, R. 1990, Nature, 345, 786
Landau, L. D. 1932, Phys. Z. Sowjetunion, 1, 285
Laor, A. 1991, ApJ, 376, 90
Lewis, K. T., Eracleous, M., & Storchi-Bergmann, T. 2010, ApJS, 187, 416
Lynden-Bell, D. 1969, Nature, 223, 690
Lynden-Bell, D., & Rees, M. J. 1971, MNRAS, 152, 461
Markowitz, A., Reeves, J. N., Miniutti, G., et al. 2008, PASJ, 60S, 277
Matsuoka, M., Piro, L., Yamauchi, M., & Murakami, T. 1990, ApJ, 361, 440
Matt, G., Perola, G. C., & Piro, L. 1991, A&A, 247, 25
Matt, G., Perola, G. C., Piro, L., & Stella, L. 1992, A&A, 257, 63
Misner, C. W., Thorne, K. S., & Wheeler, J. A. 1973, San Francisco: W.H. Freeman and Co.
Mushotzky, R. F., Serlemitsos, P. J., Boldt, E. A., Holt, S. S., & Becker, R. H. 1978, ApJ, 220, 790
Nandra, K., Pounds, K. A., Stewart, G. C., George, I. M., Hayashida, K., Makino, F., & Ohashi, T. 1991, MNRAS, 248, 760
Nandra, K., George, I.M., Mushotzky, R.F., Turner, T.J. & Yaqoob, T. 1997, ApJ, 477, 602
Nandra, K., George, I. M., Mushotzky, R. F., Turner, T. J., Yaqoob, T. 1999, ApJ, 523, 17
Nandra K., O'Neill P.M., George I.M., Reeves N. 2007, MNRAS, 382, 194
Oppenheimer, J. R., & Snyder, H. 1939, Physical Review , 56, 455
Oshima, T., Mitsuda, K., Fujimoto R., Iyomoto N., Futamoto K., et al. 2001, ApJ, 563, L103
Page, K. L., O'Brien, P. T., Reeves, J. N., & Turner, M. J. L. 2004, MNRAS, 347, 316
Penrose, R. 1965, Physical Review Letters, 14, 57
Peterson, B. M. 1997, An introduction to active galactic nuclei, Cambridge University Press, Cambridge, New York
Peterson, B. M., Ferrarese, L., Gilbert, K. M., et al. 2004, ApJ, 613, 682
Piro, L., Yamauchi, M., & Matsuoka, M. 1990, ApJ, 360, L35
Popović, L.Č, Mediavilla, E. G., Muñoz, J. A., Dimitrijević, M. S., & Jovanović, P. 2001, Serbian Astronomical Journal, 164, 53
Popović, L.Č., Mediavilla, E.G., Jovanović, P., Muñoz, J.A. 2003, A&A, 398, 975
Popović, L.Č., Jovanović, P., Mediavilla, E.G., Muñoz, J.A. 2003, A&A Trans., 22, 719
Popović, L. Č., Jovanović, P., Mediavilla, E., Zakharov, A. F., Abajas, C., Muñoz, J. A., & Chartas, G. 2006, ApJ, 637, 620
Popović, L.Č., Jovanović, P., Petrović, T., & Shalyapin, V. N. 2006, Astronomische Nachrichten, 327, 981
Pounds, K. A., Nandra, K., Stewart, G. C., George, I. M., & Fabian, A. C. 1990, Nature, 344, 132
Reynolds, C. S., Nowak, M. A. 2003, Phys. Rep., 377, 389
Schneider, P. 2006, Extragalactic Astronomy and Cosmology An Introduction, Springer-Verlag GmbH: Heidelberg
Schwarzschild, K. 1916, Sitzungsberichte der Königlich-Preussischen Akademie der Wissenschaften, Sitzung vom 3. Februar 1916, 189
Shakura, N.I., & Sunyaev, R.A. 1973, A&A, 24, 337
Shu, X. W., Yaqoob, T., & Wang, J. X. 2010, ApJS, 187, 581
Stella, L. 1990, Nature, 344, 747
Sulentic, J. W., Marziani, P., & Calvani, M. 1998, ApJ, 497, L65
Tanaka, Y., Nandra, K., Fabian, A. C., Inoue, H., Otani, C., Dotani, T., Hayashida, K., Iwasawa, K., Kii, T., Kunieda, H., Makino, F., Matsuoka, M. 1995, Nature, 375, 659
Thorne, K. S. 1974, ApJ, 191, 507
Turner, T. J., George, I. M., Nandra, K., & Mushotzky, R. F. 1997, ApJ, 488, 164
Velikhov, E. P., 1959, Sov. Phys. JETP 36, 995
Wang, J., Wang, T., Zhou, Y. ApJ, 2001, 549, 891
Wald, R. M. 1984, General relativity, University of Chicago Press, Chicago
Wheeler, J. A. 1968, American Scientist, 56, 1
Wilms, J., Reynolds, C. S., Begelman, M. C., Kendziorra, E., Staubert, R., Reeves, J., & Molendi, S. 2004, Mem. Soc. Astron. Italiana, 75, 519
Yaqoob, T., George, I. M., Nandra, K., Turner, T. J., Serlemitsos, P. J., & Mushotzky, R. F. 2001, ApJ, 546, 759
Yaqoob, T., & Padmanabhan, U. 2004, ApJ, 604, 63
Yaqoob, T., Reeves, J. N., Markowitz, A., Serlemitsos, P. J., Padmanabhan, U. 2005, ApJ, 627, 156
Zakharov, A. F., Popović, L. Č., Jovanović, P. 2004, A&A, 420, 881
Życki, P. T. 2004, MNRAS, 351, 1180